JOURNAL OF MATERIALS SCIENCE 19 (1984) 3593–3601

Thermal transformations of iron(III)–nickel(II) mixed oxide gels

V. SITAKARA RAO, S. RAJENDRAN, H. S. MAITI
Department of Chemistry and Materials Science Centre, Indian Institute of Technology, Kharagpur – 721302, India

Iron–nickel mixed oxide gels have been prepared by a hydroxide co-precipitation technique and their thermal transformation has been studied by thermal analyses, X-ray diffraction and infra-red spectroscopy. Differential thermal analysis (DTA) of the hydrated ferric oxide gel indicates the presence of three exothermic peaks along with a broad endotherm. Addition of nickel oxide decreases the intensities of the exotherms and the peaks are completely absent in the samples containing more than 10 mol % of NiO. On the other hand these samples show the presence of three endothermic peaks. Thermal analysis of the sample containing 50 mol % of NiO indicates the formation of a precursor at around 185° C which changes to nickel ferrite at around 275° C. This ferrite slowly crystallizes with a broad exotherm in the range 280 to 550° C.

1. Introduction

Ferric oxide, besides being extensively used in the paint industry, possesses useful electrical, magnetic and catalytic properties. Doping with other oxides has a significant effect on these properties. Both pure and mixed oxides are usually prepared by thermal decomposition of the precipitated gels. The characteristics of the thermal transformation of pure and mixed ferric oxide gels have, therefore, been studied extensively by various investigators using different experimental techniques [1–10]. The nature of the transformations strongly depends on the method of preparation and other experimental conditions. Caslaska *et al.* [11] observed a continuous dehydration behaviour of the gel which had been prepared in the presence of sulphate ions and a discontinuous behaviour for the gel prepared in the presence of nitrate ions. Mackenzie [1] tried to establish the relationship between the temperature of precipitation and the temperature at which the highest dehydration rate occurs. The relationship between the dehydration temperature and the ageing time as well as the pH of the solution during ageing have also been studied by many investigators [3, 5–8].

Thermal characteristics of the hydrated ferric oxide gel prepared by the authors under a definite set of experimental conditions has been reported earlier [12]. The nature of the primary particle of the gel is found to be α-FeOOH, which crystallizes completely above 210° C and transformed to α-Fe_2O_3 with an exothermic peak at 315° C. The crystallite size of the α-Fe_2O_3 formed is found to be around 7 nm but changed to nearly 30 nm with a sharp exotherm at about 430° C.

In this paper the authors are reporting the characteristics of thermal decomposition of the iron–nickel mixed oxide gels for which practically no information is available in the literature. For comparison, the thermal characteristics of nickel hydroxide are also presented.

2. Experimental procedure

The nickel hydroxide was prepared by adding 0.5 molar nickel nitrate (BDH-Analar) solution to a freshly prepared and continuously stirred 4 N sodium hydroxide (S. Merck – G.R) solution kept at room temperature (30° C). The precipitation was over within 5 to 10 minutes. The pH, which was measured with a digital pH meter, was adjusted finally to 12.5 by further addition of 4 N sodium hydroxide solution. The nickel hydroxide precipitate was aged for an hour at 100° C by keeping it in a water bath and then at room tem-

0022–2461/84 $03.00 + .12

TABLE I Sample code with corresponding nickel oxide concentration

Code	Concentration of NiO (mol%)
FN0	0
FN0.5	0.5
FN1	1
FN2	2
FN5	5
FN10	10
FN20	20
FN50	50
FN100	100
FNM10	10
FNM20	20
FNM50	50

perature for two hours. The precipitate was washed repeatedly with distilled water until free from alkali and then the sample was dried in an air oven for 12 h at 110° C.

For the preparation of iron–nickel mixed oxide gels, appropriate amounts of ferric ammonium sulphate (E. Merck – G.R) and nickel nitrate were dissolved in 100 ml of distilled water. The concentration of the mixed metal ions in the solution was approximately 0.5 molar. The solution was then added to 50 ml of freshly prepared highly concentrated sodium hydroxide solution (4N) kept at room temperature. The solution was continuously stirred with a mechanical stirrer during precipitation. The pH of the solution was finally adjusted to 12.5 by further addition of 4N sodium hydroxide solution. Other experimental conditions were similar to those used for the preparation of nickel hydroxide and hydrated ferric oxide gel [12]. The sample codes with corresponding composition are given in Table I. In this, FN indicates the co-precipitated samples of iron and nickel oxide gels and FNM represents the mechanical mixture of oven dried iron oxide gel and nickel hydroxide. The number in the code indicates the mol % of NiO present in the sample.

Thermal analyses of the oven dried samples of iron, nickel and iron–nickel mixed oxide gels were carried out using a derivatograph (MOM-Hungary) with a heating rate of 10° C min^{-1}. 200 mg of the sample was taken for each run.

The infra-red spectra were taken with a Perkin-Elmer 237B model spectrophotometer in the range 4000 to 625 cm^{-1} using nujol as a mulling agent. In all the cases nearly 5 mg of the sample was made into a paste with nujol and this was taken as a thin layer between sodium chloride plates to obtain the spectra.

X-ray diffraction experiments were carried out in a DRON II (USSR) X-ray diffractometer using Fe$K\alpha$ radiation with a power rating of 30 kV and 15 mA. A scanning speed of 2° min^{-1} was used for this purpose.

3. Results

The results of differential thermal analysis of the mixed oxide gels containing up to 10 mol% of NiO along with those of pure ferric oxide gel and nickel hydroxide are shown in Fig. 1. The FNO sample represents a broad endothermic peak around 130° C. Along with this endotherm, three exothermic peaks are also present at 210, 315 and 430° C (Peak Nos. I, II and III respectively). With increasing concentration of NiO up to 10 mol% neither the temperature nor the intensity of the first endothermic peak of the mixed oxide gels vary significantly. Nor do the first two exothermic peak temperatures also vary appreciably with increasing nickel oxide concentration, but the third exothermic peak (No. III) is continuously shifted to higher temperatures as the nickel oxide content is increased. For example, the sample FN5 (sample containing 5 mol% of NiO) shows this exothermic peak at 510° C. The intensities of all the exothermic peaks gradually decrease up to 5 mol % of nickel oxide and all the exothermic peaks are completely absent in the sample containing 10 mol% of nickel oxide (FN10). The DTA curve of FN100 (pure nickel hydroxide) indicates a small endothermic effect around 115° C and a sharp endotherm at 300° C immediately followed by an exothermic peak at 330° C. The DTG results (Fig. 2) of all these samples show two minima at temperatures of about 120 and 300° C, which are very close to those observed in DTG of pure iron oxide gel.

Samples containing 20 and 50 mol% of NiO behave quite differently from those containing lower concentrations of NiO. Thermal analyses results of these samples are presented separately in Figs. 3 and 4. The DTA plots of both the samples show three endothermic peaks and the peak temperatures are found to be around 100, 275, 370° C and 100, 185, and 275° C respectively. In addition to these endothermic peaks the sample FN50 also shows a broad exothermic peak in the temperature range 280 to 550° C (Fig. 4). No such exothermic peak is, however, observed in the sample

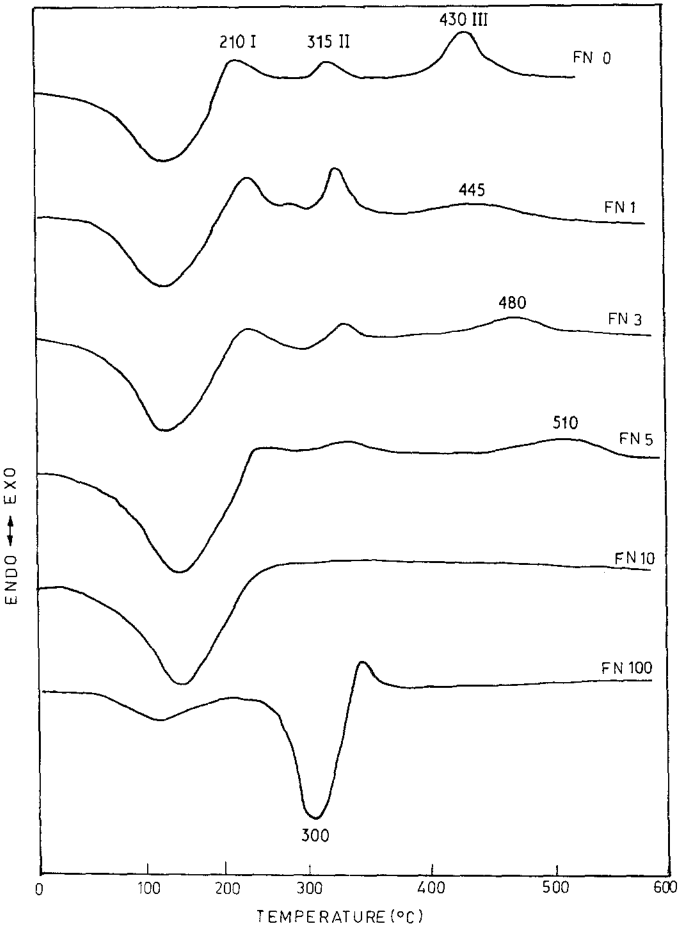

Figure 1 DTA of iron(III)–nickel(II) mixed oxide gels.

FN20 (Fig. 3). The DTG results of these samples also show three peaks almost at the same temperatures as those of the endothermic DTA peaks of the respective samples. The DTA curves of the mechanical mixtures of the ferric oxide gel and the nickel hydroxide containing 10, 20 and 50 mol% of nickel oxide (FNM10, FNM20 and FNM50) along with pure ferric oxide gel (FNO) are given in Fig. 5. The behaviour of the FNM10 is almost identical to that of the pure ferric oxide gel as there is no change in any of the peak temperatures of this sample compared to the DTA peaks of ferric oxide gel. However, in the case of the sample FNM20, the third exothermic peak is shifted to a higher temperature (from 430 to around 510° C) and this exothermic effect is completely absent in the sample FNM50.

4. Discussion

Before discussing the transformational characteristics of the mixed oxide gels, it may be useful to consider the behaviour of pure nickel hydroxide. The DTA of nickel hydroxide (Fig. 1) shows a small endothermic peak at around 115° C which is due to the removal of loosely bound adsorbed water. The second strong endotherm at 300° C is due to the removal of constitutional water associated with the formation of nickel oxide which, however, remains in the amorphous state, as indicated by the absence of any X-ray diffraction peak. The two-step dehydration process is also indicated by the presence of two DTG peaks, the temperatures of which exactly coincide with those of the DTA peaks (Fig. 2). The fact that the weight of the sample remains practically constant beyond 300° C is indirect evidence that the amorphous phase formed at this temperature is nothing but nickel oxide.

From TG results (not given), the total weight loss of the nickel hydroxide sample is found to be about 29% and accordingly the composition of the oven dried nickel hydroxide sample can be written

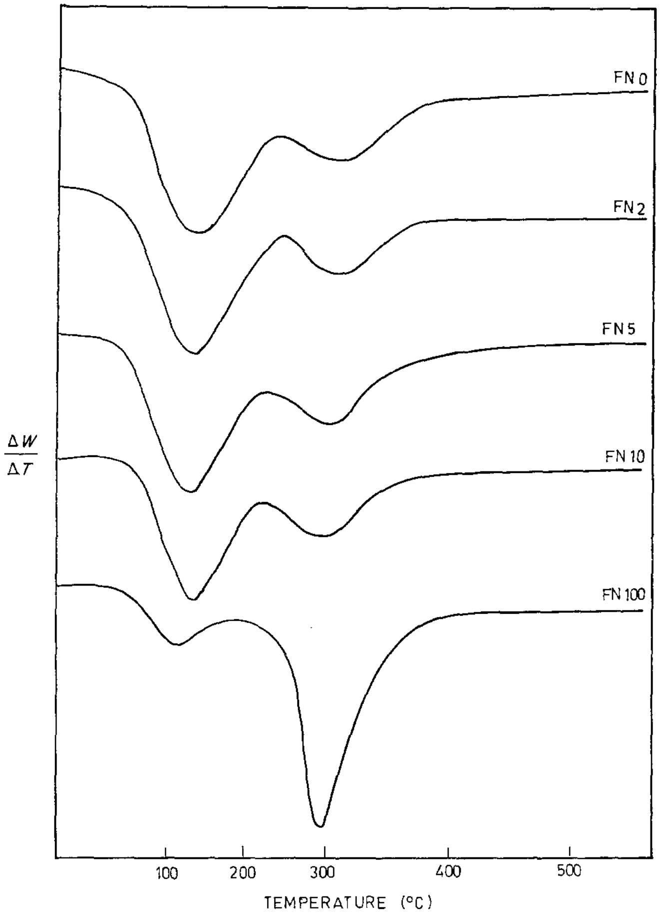

Figure 2 DTG of iron(III)–nickel(II) mixed oxide gels.

as $Ni(OH)_2 0.5H_2O$. X-ray diffraction of dehydrated nickel hydroxide samples, in this investigation, show the crystalline nickel oxide peaks only above 380° C, indicating that the exothermic DTA peak observed at 330° C is related to an amorphous-to-crystalline transformation. Thermal analysis of nickel hydroxide has been carried out earlier by many investigators [13, 14] and most of them have reported the existence of these endothermic peaks. The only exception is Rode [15], who observed an exothermic peak along with an endotherm. He explained the origin of the exotherm as being due to a crystallographic transformation of rhombohedral to cubic form of nickel oxide. In the present sample, however, no such phase transformation is detected. All the samples in this case show only the cubic form of the oxide.

The first two exothermic peaks of ferric oxide gel are due to the crystallization of α-FeOOH and the transformation of α-FeOOH to $\alpha\text{-}Fe_2O_3$ [12]. Therefore, the decrease in intensity of these two peaks with increasing concentration of NiO for the samples FN1 to FN10 (Fig. 1) may be either due to (i) a compensating effect between the two exotherms of pure ferric oxide gel and the endotherm of the nickel hydroxide, all of which are present in the same temperature region, or (ii) because of the fact that the nickel ions create a condition which is unfavourable for the formation of α-FeOOH and therefore there may be a gradual decrease of α-FeOOH concentration with increasing NiO content.

If the first factor alone is responsible for the decrease in intensities of the exothermic peaks, similar effects should have been observed in the DTA results for the mechanical mixtures containing both ferric oxide gel and nickel hydroxide. But the DTA curves of FNM10 and FNM20 samples do not show any significant decrease in intensities of the two exothermic peaks, as observed in Fig. 5. The compensating effect is, however, evident only in the sample FNM50 which contains a much larger quantity of $Ni(OH)_2$ (50 mol %). It may

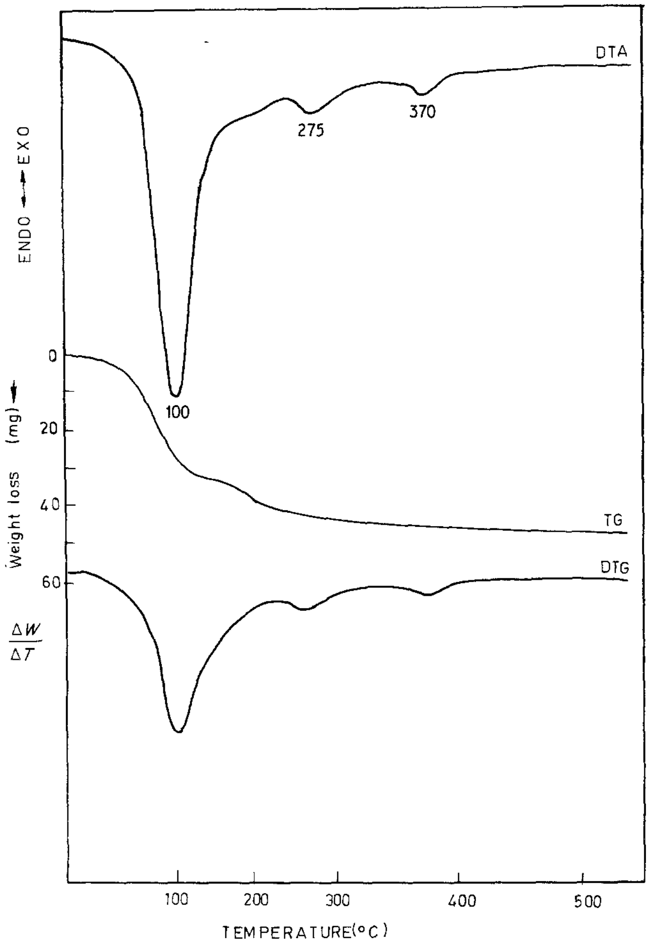

Figure 3 DTA, TG and DTG of FN20 sample.

therefore be concluded that the decrease in the intensities of the first two DTA peaks of the co-precipitated samples is not due to any compensating effect but is the result of the formation of lesser quantities of α-FeOOH as predicted in the second point mentioned above. Further confirmation of this view is obtained from the infra-red spectra of the mixed oxide gels (oven dried) presented in Fig. 6. It shows that the two sharp peaks at 900 and 800 cm^{-1} which correspond to the O–H...O bending modes of α-FeOOH are present only in the samples containing up to 2 mol% of NiO [16, 17]. Above this concentration these absorption peaks are completely absent, indicating that the amount of the α-FeOOH present in those samples is negligible. These results clearly indicate that the presence of nickel ions in the solution prevents the formation of α-FeOOH in the ferric oxide gel.

The minima (around 120 and 300° C) observed in DTG curves of iron–nickel mixed oxide gels (Fig. 2) may be explained as due to the removal of loosely bound adsorbed water and the formation of the corresponding oxides from the gels respectively.

The third exothermic peak at 430° C (peak No. III of Fig. 1) is due to the sudden increase of crystallite size within a relatively narrow range of temperature [12]. The gradual decrease of intensity of this peak with a shift in the peak position with increasing concentration of nickel oxide can be explained on the basis of one or both of the following reasons:

1. There may be a formation of solid solution between Fe_2O_3 and NiO resulting in a change in the initial crystallite size and surface area of the sample.

2. There may be a mutual interaction between the oxides to form a new compound like nickel ferrite. Presence of a second phase either in the form of nickel ferrite or free nickel oxide, which may be present if there is no interaction between

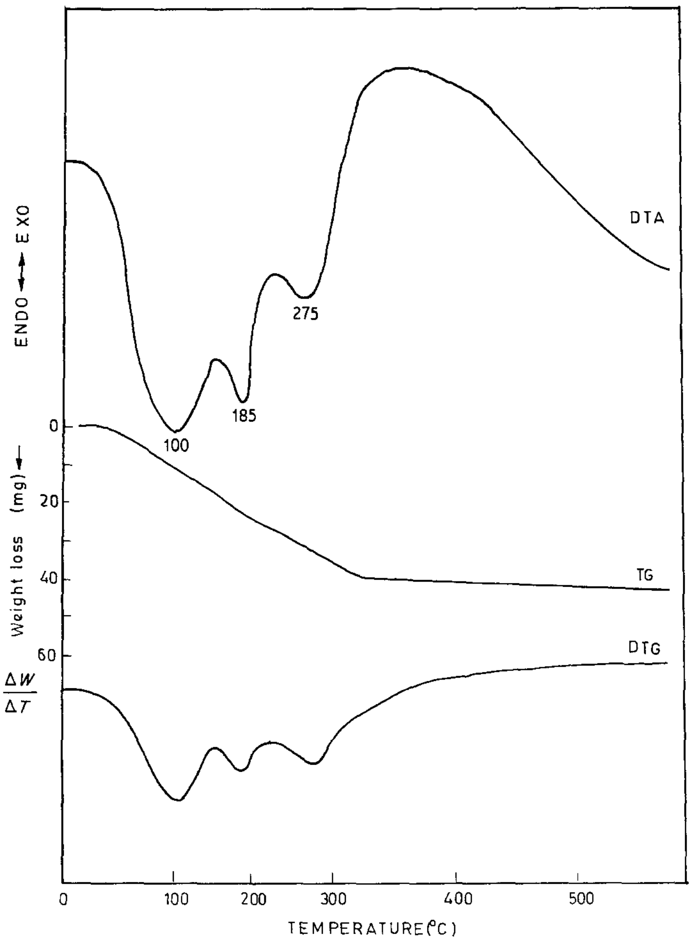

Figure 4 DTA, TG and DTG of FN50 sample.

Fe_2O_3 and NiO, may have a protective action preventing the growth of the iron oxide particles.

As is discussed elsewhere [18], the solubility limit of NiO in Fe_2O_3, detected from X-ray and magnetic susceptibility measurements, is only 2 mol% when the co-precipitated gels are heated up to 550° C. Above this concentration formation of nickel ferrite has been detected, but none of the samples contained nickel oxide as a second phase. Since the third exothermic peak of the mixed oxide gels continuously shifts to higher temperatures even beyond 2 mol% of NiO, formation of the solid solution may not be the only factor responsible for this shift. However, the solid solubility can be considered as the major factor responsible for the peak shift in the concentration region 0 to 2 mol% of NiO because the samples with such low concentration of NiO do not contain any second phase either in the form of free NiO or $NiFe_2O_4$. In the samples containing higher concentrations of NiO, the protective action of the nickel ferrite phase is one of the possible reasons for the observed shift in the peak positions and the decrease of peak intensities. This is partly supported by the observation that the DTA results of the samples prepared by mechanical mixing of the ferric oxide gel and nickel hydroxide also show a decrease of intensity and a shift in the peak temperature with increasing concentration of NiO, particularly beyond 10 mol% NiO. It may also be possible that a thermodynamically metastable solid solution exists even beyond the 2 mol% NiO limit, particularly at lower temperatures, and that small amounts of such solid solution are preserved for a short time even at higher temperatures. Such a situation would also account for the observed peak shifts in FN3 and FN5 of Fig. 1.

The DTA curves of the 50 mol% sample (Fig. 4) show the presence of three endothermic peaks along with a very broad exothermic effect. All the three endothermic processes are associated with weight losses as indicated by the three minima in

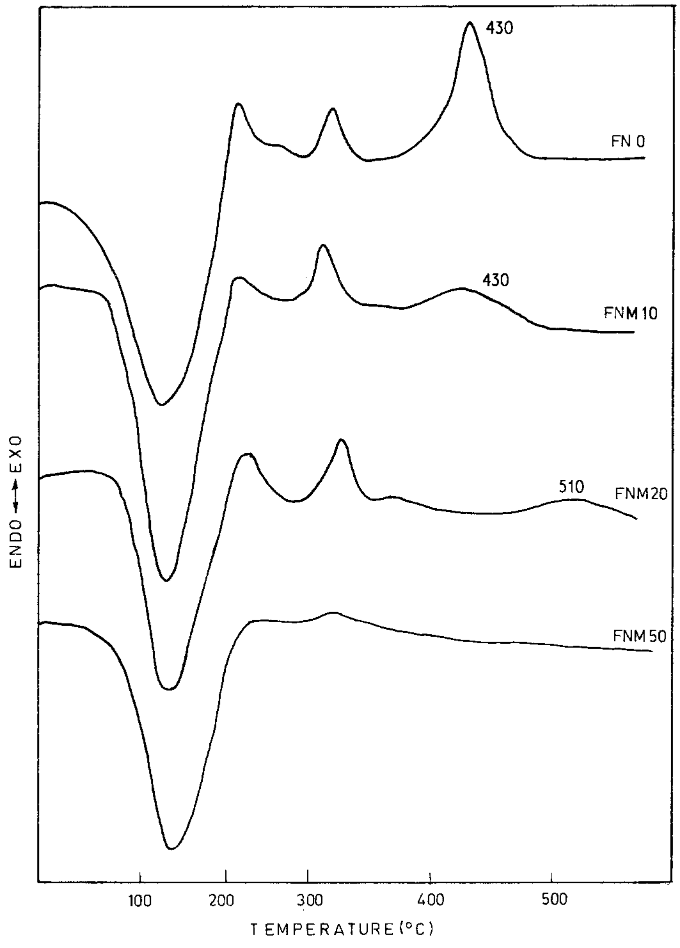

Figure 5 DTA curves of mechanical mixtures of ferric oxide gel and nickel hydroxide.

the DTG plot. As usual, the first endotherm arises from the removal of loosely bound adsorbed water. The X-ray diffraction analysis of this sample heated to different temperatures shows the presence of crystalline nickel ferrite above 400° C and the sample heated below this temperature is amorphous with respect to X-rays. This observation clearly shows that the broad exothermic effect is due to the slow crystallization of nickel ferrite which might have been formed in the amorphous state at a lower temperature, most probably during the third endothermic process (275° C). This endothermic peak is associated with a weight loss of nearly 6.4%, which indicates that each mole of nickel ferrite is associated with nearly a mole of water below this temperature. Therefore, the second endothermic effect at 185° C may be due to the formation of a precursor having the formula $NiFe_2O_4 \cdot H_2O$. This precursor is converted to nickel ferrite during the third endothermic process.

From the TG results, the total weight loss of this sample is found to be 25%, which corresponds to 3.6 molecules of water per molecule of the nickel ferrite composition. The weight loss corresponding to the first and the second endothermic processes are 12.0 and 6.6% respectively. Based on these results the thermal transformation of this sample can be represented as:

$$Fe_2O_3 \cdot NiO \cdot 3.6H_2O \xrightarrow{100^\circ C} Fe_2O_3 \cdot NiO \cdot 2.1\,H_2O$$

$$\xrightarrow{185^\circ C} NiFe_2O_4 \cdot H_2O \xrightarrow{275^\circ C} \underset{\text{(amorphous)}}{NiFe_2O_4}$$

$$\xrightarrow{>400^\circ C} \underset{\text{(Crystalline)}}{NiFe_2O_4}$$

Earlier Arora *et al.* [19–22] reported the formation of similar spinel precursors in the mixed oxide systems like $ZnO-Al_2O_3$, $MgO-Fe_2O_3$ and $MgO-Cr_2O_3$ at a lower temperature with endothermic effects transforming to the corresponding

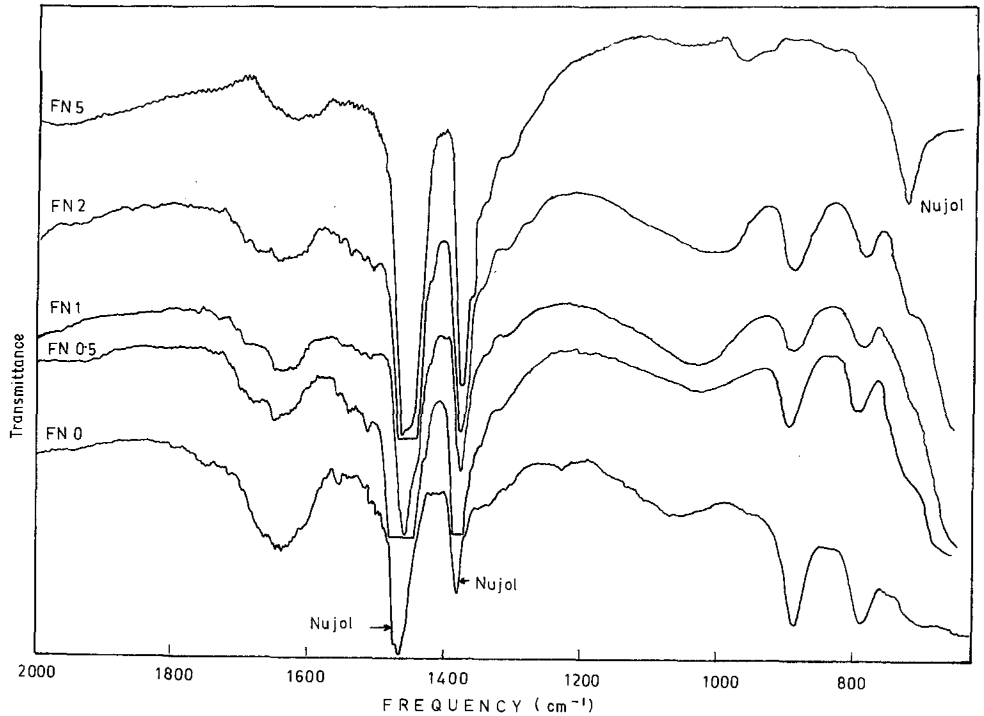

Figure 6 Infra-red spectra of iron–nickel mixed oxide gels dried at 110° C.

spinels at relatively higher temperatures. But no such precursor formation and the simultaneous presence of the three endothermic peaks have been reported for the NiO–Fe_2O_3 system. Stuijts [23] reported the formation of nickel ferrite at about 300° C from the co-precipitated iron–nickel oxalates, whereas others [24] have reported the formation of the same phase at about 460° C with an endothermic effect from the co-precipitated hydroxides. They did not, however, observe any exothermic effect corresponding to the crystallization of the amorphous phase.

The sample containing 20 mol% of NiO (FN20) also shows the presence of three endothermic peaks and the DTG result shows the presence of three peaks indicating that the weight loss takes place in three different stages (Fig. 3). The second and third peak temperatures (275 and 370° C, respectively) are much higher than that of the 50 mol% sample. These endothermic peaks may be related to (i) the removal of physically adsorbed water, (ii) the formation of precursor to the spinel and the formation of the oxides, and (iii) the formation of spinel ferrite. The higher peak temperature of the third endothermic peak (370° C) may be due to the presence of excess α-Fe_2O_3. The X-ray diffraction pattern of a sample of this composition heated to 550° C shows the presence of both nickel ferrite and α-Fe_2O_3.

5. Conclusions

These results indicate that the presence of nickel ions in ferric ion solution creates an unfavourable condition for the formation of α-FeOOH. In fact, the mixed oxide gels containing more than 2 mol% of NiO do not show the presence of α-FeOOH. DTA results suggest the formation of a solid solution between Fe_2O_3 and NiO, at least up to 2 mol% of NiO, and nickel ferrite formation above this mol% of NiO.

The sample with a composition of 50 mol% NiO shows the formation of a nickel ferrite precursor at around 185° C with a composition $NiFe_2O_4 \cdot H_2O$ which is later converted to amorphous nickel ferrite at about 275° C. This phase is finally converted to a crystalline variety above 400° C.

References

1. R. C. MACKENZIE, *Nature* **164** (1949) 244.
2. J. L. KULP and A. F. TRITES, *Amer. Mineral.* **36** (1951) 23.
3. M. A. GHEITH, *Amer. J. Sci.* **250** (1952) 677.
4. S. J. GREGG and K. J. HILL, *J. Chem. Soc. (London)* (1953) 3945.

5. R. C. MACKENZIE and R. MELDAU, *Mineral. Mag.* **32** (1959) 153.
6. L. G. BERG, K. P. PRIBYLOV, V. P. EGUNOV and R. A. ABDURÅKHMANOV, *Russ. J. Inorg. Chem.* **14** (1969) 1211.
7. M. SORRENTINO, L. STEINBRECHER and F. HAZEL, *J. Colloid Interface Sci.* **31** (1959) 307.
8. E. P. TSYMBAL, S. I. SMYSHLYAER and L. M. DVORNIKOVA, *Russ. J. Inorg. Chem.* **15** (1970) 1653.
9. K. KAUFFMAN and F. HAZEL, *J. Colloid Interface Sci.* **51** (1975) 422.
10. I. P. SARASWAT, A. C. VAJPEI, V. K. GARG, V. K. SHARMA and N. PRAKASH, *ibid.* **73** (1980) 373.
11. V. CASLASKA, V. FREI and A. BLAZEK, *Coll. Czech. Chem. Commun.* **27** (1962) 2168.
12. S. RAJENDRAN, V. SITAKARA RAO and H. S. MAITI, *J. Mater. Sci.* **17** (1982) 2709.
13. W. M. KEELY and H. W. MAYNOR, *J. Chem. Eng. Data* **8** (1963) 297.
14. M. LE VAN MY, *Bull. Soc. Chim. (France)* (1964) 545.
15. E. YA RODE, *Z. Neorg. Khim* **1** (1956) 1430.
16. A. A. VAN DER GIESSEN, *Phillips Res. Rep. Suppl.* **12** (1968).
17. S. RAJENDRAN, V. SITAKARA RAO and H. S. MAITI, *Trans. Ind. Ceram. Soc.* **41** (1982) 97.
18. *Idem* (to be published) in *J. Solid State Chem.*
19. B. R. ARORA, R. K. BANERJEE, T. S. R. PRASAD RAO, N. K. MANDAL, N. B. BHATTACHARYYÀ and S. P. SEN, *Thermochim. Acta* **6** (1973) 11.
20. B. R. ARORA, R. K. BANERJEE, T. S. R. PRASAD RAO, N. K. MANDAL, N. C. GANGULI and S. P. SEN, *ibid.* **7** (1973) 25.
21. B. R. ARORA, B. N. SINGH and R. K. BANERJEE, *J. Therm. Anal.* **13** (1978) 449.
22. B. N. SINGH, R. K. BANERJEE and B. R. ARORA, *ibid.* **18** (1980) 5.
23. A. L. STUIJTS, Proceedings of the 5th International Conference on the Science of Ceramics, April 20–23, Ronnely Brum., Sweden, 1969, edited by C. Brosset and E. Knoop (Swedish Institute for Silicate Research, 1970) p. 335.
24. F. DOMKA, Z. DUDZIK and M. GASIOREK, *React. Kinet. Catal. Lett.* **2** (1975) 171.

Received 12 October 1983
and accepted 24 January 1984